Sinuous pockmark belt as indicator of a shallow buried turbiditic channel on the lower slope of the Congo basin, West African margin

Aurélien Gay, M Lopez, Pierre Cochonat, Nabil Sultan, Eric Cauiquil, Frederic Brigaud

Sinuous pockmark belt as indicator of a shallow buried turbiditic channel on the lower slope of the Congo basin, West African margin

A. GAY[1,2,*], M. LOPEZ[2], P. COCHONAT[3], N. SULTAN[3], E. CAUQUIL[4] & F. BRIGAUD[4]

[1]*Université de Lille I, Laboratoire Sédimentologie et Géodynamique, FRE 2255, Bât SN5, 59655 Villeneuve d'Ascq, France.*

[2]*Université de Montpellier II, Laboratoire Géophysique Tectonique et Sédimentologie, CC60, Bât 22, place E. Bataillon, 34095 Montpellier cedex, France*

(e-mail: gay@elstu-univ-montp2.fr)

[3] *IFREMER, Institut Français de Recherche et d'Exploitation de la MER, Département Géosciences Marines, Laboratoire Environnements Sédimentaires, BP70, 29280 Plouzané, France*

[4] *Total-Fina-Elf, 64018 Pau Cedex, France*

Abstract: Pockmarks on the slope of the Lower Congo Basin are distributed along a meandering band on seafloor coincident with a shallow buried palaeochannel imaged from the 3D-seismic database. Each pockmark originates systematically at the channel-levee interface and the seafloor expression of the palaeochannel's sinuosity is mimicked by the sinuous trend of pockmarks. 3D-seismic on the slope, calibrated by biostratigraphic data from cores of the Leg ODP 175, indicate a seaward decrease of the sedimentation rate. We suggest that this condition induces a differential loading of the hemipelagic cover over the palaeochannel and propose a model for episodic dewatering of fluids trapped in the buried turbiditic channel. The consequence is a fluid flow caused by a longitudinal pressure gradient along the buried channel. A hydromechanical model proposed for the formation of shallow pockmarks indicates that the sedimentation rate cannot generate the overpressure required for pockmark formation on the seafloor. Therefore, it is suggested that hydrocarbon migration from deeper overpressured reservoirs is added to the pore fluid pressure in the shallow subsurface sediments. Horizontal drainage by the turbiditic palaeochannel and vertical migration along many vertical conduits (seismic chimneys) probably initiated at shallow subbottom depth. It is concluded that these shallow processes have important implications for fluid migration from deeply buried hydrocarbon reservoirs.

Pockmarks were first reported on sidescan records from the Scotian Shelf by King & MacLean (1970). Since their initial identification pockmarks have been widely reported during offshore hydrocarbon exploration and scientific surveys at water depths ranging from 30 m to over 3000 m (see Josenhans *et al.* 1978; Werner 1978; Hovland 1981; Whiticar & Werner 1981; Hovland *et al.* 1984; Solheim & Elverhoi 1993; Baraza *et al.* 1999 for a detailed review). They generally appear in unconsolidated fine-grained sediments as cone-shaped circular or elliptical depressions ranging from a few metres to 300 m or more in diameter and from 1 m to 80 m in depth.

Pockmarks generally concentrate in fields extending over several square kilometres where they often appear as isolated patches named single pockmarks or 'eyed pockmarks' (Hovland & Judd 1988). In some cases, they have been identified along straight or circular lines correlated with glaciomarine tills (Josenhans *et al.* 1978; Whiticar & Werner 1981; Kelley *et al.* 1994) or suggesting a structural control for fluid flow (Eichhubl *et al.* 2000). In particular, structural surfaces along bedrock (Shaw *et al.* 1997), salt diapirs (Taylor *et al.* 2000) and faults and faulted anticlines (Boe *et al.* 1998; Soter 1999; Vogt *et al.* 1999; Eichhubl *et al.* 2000) create pathways for fluid migration. These observations suggest that discontinuities or unconformities are much more effective for fluid migration than a simple seepage through the sedimentary column (Abrams 1992; Brown 2000) and are responsible for pockmarks development (Abrams 1996; Orange *et al.* 1999). The crater-like nature of pockmarks suggests the erosional power of fluid venting, commonly related to an overpressured buried reservoir of biogenic gases, thermogenic gases or oil, interstitial water, or a combination of the three. Many authors attempted to establish a link on seismic sections between seafloor pockmarks and

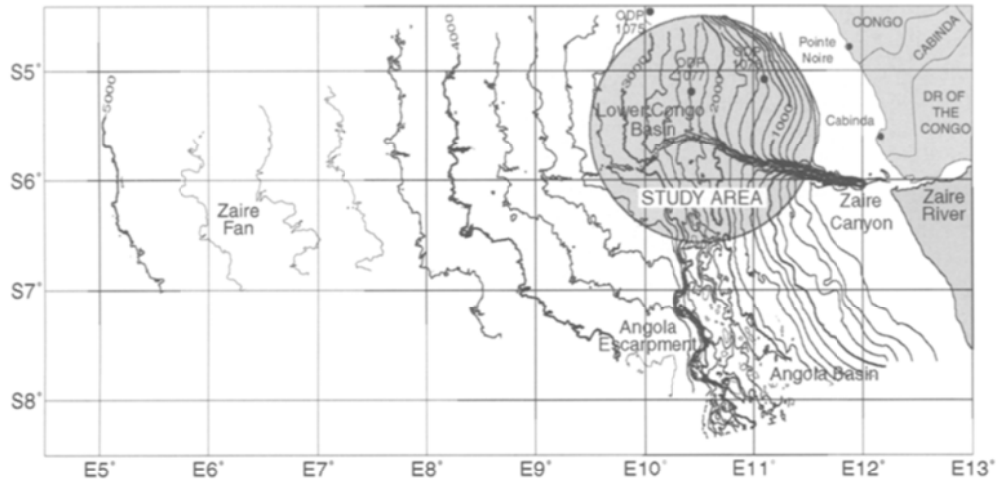

Fig. 1. Bathymetric map of the Zaire turbidite system, extending from the Zaire estuary to the deep sea fan. The shaded circle represents the study area in the Lower Congo Basin. The three sites of the Leg ODP175 in this zone are indicated.

buried anomalies such as seismic chimneys (Heggland 1998) and acoustically 'blanked' layers, which are interpreted as gas accumulations (Yun *et al.* 1999) or gas-charged sediments (Hovland *et al.* 1984; Hempel *et al.* 1994). Because of the nature of fluids expelled, pockmarks may represent open-windows above the petroleum system and could be valuable indicators for deeper reservoir strategy. On the slope of the Lower Congo Basin, pockmarks are not randomly distributed, but always associated with fault zones, salt diapirs or gas hydrates intervals. Moreover, detailed analysis of bathymetric maps and 3D-seismic data permitted to characterize a sinuous belt of pockmarks that mimicked a shallow buried meandering channel of Pliocene age acting as a horizontal drain for interstitial fluids. This paper focuses on morphological aspects, distribution and hydromechanical model of this new kind of pockmarks. The later has to be regarded as an indicator of overpressure at shallow subsurface levels that can initiate fluidization features in unconsolidated sediments, if the seepage forces due to fluid flow are larger than its own weight.

Geological setting

The West African passive margin was initiated during the opening of the South Atlantic Ocean at Early Cretaceous (130 My) (Jansen *et al.* 1984; Marton *et al.* 2000). Subsequent to large accumulations of evaporites (up to 1000 m) during the Aptian, the post-rift stratigraphy is characterized by two distinct seismic architectures that reflect a major change in ocean circulation and climate:

(1) From Late Cretaceous to Eocene time an aggradational carbonate/siliciclastic ramp develops in response to low-amplitude/low-frequency sea-level changes and stable climate (i.e. greenhouse period, Bartek *et al.* 1991; Seranne *et al.* 1992; Seranne 1999).
(2) From Oligocene time to Present, sedimentation was dominated by the progradation of a terrigenous wedge that reflects high-amplitude/high-frequency sea-level changes and an alternating drier and wetter climate (i.e. ice-house period; Seranne 1999).

During the icehouse period, due to the global climate cooling the increased terrigenous input to the Atlantic Ocean rejuvenated deposition of a large tubiditic fan off Congo and Angola slopes directly fed by the Zaire River (Brice *et al.* 1982; Reyre 1984; Uchupi 1992; Droz *et al.* 1996). The total thickness of the turbidite fan ranges from 8 to 10 km-thick and extends from the Zaire estuary down to 4000 m water depth (Fig. 1). During flooding stages, the Zaire river discharged high density bed load into the submarine canyon that originates directly at the river mouth, to feed a large sinuous channel-levee system, far onto the lower fan (Jansen *et al.* 1984; Uenzelmann-Neben 1998; Savoye *et al.* 2000). Only fine materials, not confined to the canyon, are delivered to the Lower Congo Basin (LCB) from riverine plumes (Cooper 1999). This suspended terrigenous material is mixed with hemipelagic sediments on the continental shelf and slope to feed the 2000–3000 m thick progradational wedge that progressively overlays the abandoned turbiditic sandy-channels at the base of the slope. During the ODP Leg 175 (1998),

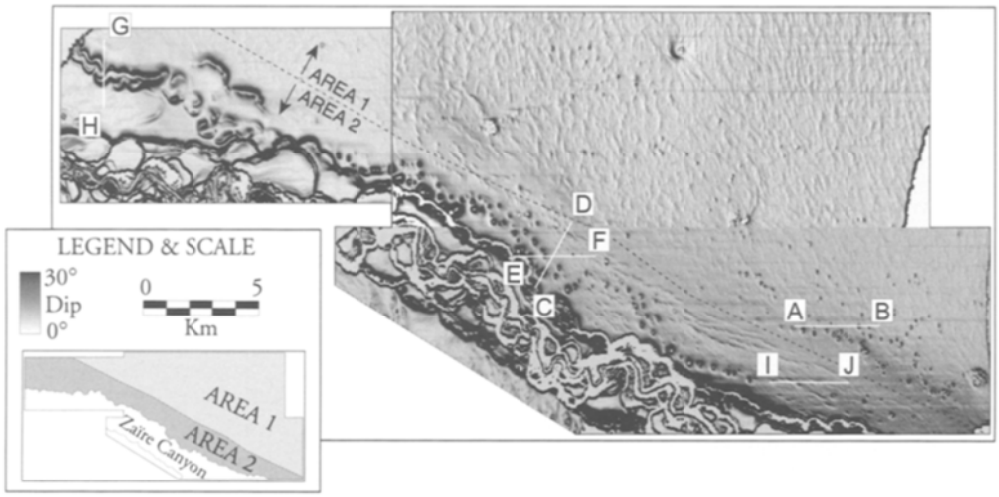

Fig. 2. Seafloor dip map in the study area. The grey-scale ranges from 0° in white (horizontal surfaces) to 30° in black (sloping surfaces). The white lines indicate seismic profiles shown in the following figures. Pockmarks are not evenly distributed on the seafloor: Area 1 is characterized by small pockmarks associated with underlying gas hydrates or diapirs, and Area 2 shows a high concentration of larger pockmarks along a sinuous belt on seafloor (see text for details).

three sites were drilled at various positions from the shelfbreak (sites 1075, 1076 and 1077), which supplied new information about the nature and age of these sediments. Biostratigraphical analyses indicate an overall continuous hemipelagic settling for Mid-Pliocene sediments occurring at a rate of about 12 cm/k.y (Giraudeau *et al.* 1998).

Data and methods

This study was primarily based on a 3D-exploration seismic dataset acquired by the Total-Fina-Elf oil company and combined with a bathymetric map and a 2D seismic Pasisar profile (see below for details) acquired during the ZAIANGO project. One of the main objectives of the ZAIANGO project was to better understand the Quaternary history of the Zaire fan (Savoye *et al.* 2000). Additional data from the Leg ODP175 on the West African Margin provided useful information on stratigraphy, sedimentation rates and mechanical properties of sediments (Wefer *et al.* 1998*b*).

The bathymetric map was acquired with a Simrad EM12 dual multibeam. Complementary data have been collected more recently with the Simrad EM300 dual multibeam and provided higher vertical and lateral resolution for acquisition in water depth less than 3500 m. The profile CD (Fig. 4) was obtained with the PASISAR system. The PASISAR is a deep seismic streamer towed behind a conventional SAR system developed by IFREMER for high-resolution studies in water depths ranging from 200 to 6000 m (Savoye *et al.* 1995).

The 3D-dataset selected for this study covers an area of 592 square kilometres with a line spacing of 12.5 m and a CDP distance of 12.5 m. They were loaded to a station and interpreted with the SISMAGE software developed by Total-Fina-Elf. 3D seismic imagery allows extraction of continuous horizons by propagation in the 3D block and attribute calculation (Kidd 1999).

Description of pockmarks on the Congo-Angola slope

Pockmarks in the Lower Congo Basin seem randomly distributed (Fig. 2). We observed more than 250 pockmarks in the study area, with an average density of 0.42 pockmarks per km. They range from 100 m up to 800 m in diameter and from a few metres to 40 m in depth. Most of them have a circular shape in plan view, but the largest pockmarks are elongated in one main direction. Detailed observations show that these large pockmarks are composite features.

The dip map of the seafloor of the investigated area extracted from the 3D-seismic (Fig. 2) delineates two main zones of pockmarks characterized by their distribution shape, size and density. Area 1 is characterized by patches or isolated small pockmarks that extend on a large domain of the northern slope of the Zaire canyon; as opposed to Area 2,

where large pockmarks are distributed in a sinuous belt at the right bank of the Zaire canyon. These two domains are clearly associated with different buried structures; First, the pockmarks of Area 1 that are of more conventional origin are described, focusing on the sinuous pockmark belt of Area 2 and the link with a subsurface channel is discussed.

Pockmarks related to gas hydrates and salt diapirs (Area 1)

Area 1 is characterized by small circular pockmarks, ranging from 100 m to 300 m in diameter, and from a few metres to a maximum of 20 m in depth (Fig. 2). They are unevenly distributed and their abundance varies considerably within the area. In particular, pockmarks develop in areas covered by 1 to 3 km regularly spaced linear depressions. These furrows have a north/south orientation, perpendicular to the regional slope with about 1 km in length and have an average depth of 5 m; they are interpreted as regular deformation by creeping of the superficial slope sediments.

Numerous seismic profiles through pockmarks show two superposed acoustic anomalies, vertically elongated under the pockmarks (Fig. 3). The shallowest anomaly is ovoid in shape with depressed high-amplitude reflectors interpreted as a reduction of the seismic velocities (pull-down effects) through a gas-charged column. Such acoustic anomalies are also called seismic chimneys and could be indicative of fluid flow from deeper levels (Hempel *et al.* 1994; Tingdahl *et al.* 2001). The deepest anomaly characterized by acoustic turbidity corresponds to an inverted cone shape, marked by a fadeout of the reflectors. On both sides of this region the bright reflectors shift upward. Profile AB (Fig. 3) shows a high-amplitude reflection parallel to the seafloor located at 250 ms TWT. This is a Bottom Simulating Reflector (BSR), which is often considered as the lower thermodynamic limit of the gas hydrates stability zone (Shipley *et al.* 1979). BSR's are characterized by the reversed polarity compared to the seafloor reflection, indicating a downward reduction of seismic impedance and therefore of seismic velocity. This contrast in impedance is probably due to the presence of free gas entrapped below the gas hydrate stability zone and the BSR can be considered as the interface between high-velocity gas hydrates and the underlying gas-charged sediments of low acoustic velocity. On this profile, the BSR is deflected upward directly beneath the pockmark depressions, suggesting a localized positive heat flow anomaly. This dome-shaped anomaly could be due to an ascending movement of fluids through the sedimentary column.

Several giant circular depressions with a diameter of 1000 m also occur within Area 1. They correspond to the imprint on the seafloor of a normal faulted network, due to the collapse above the diapir crest (Stewart 1999). Similar diapir pockmarks and BSR's offshore Nigeria have been discussed by Hovland *et al.* (1997), Heggland (1997) and Graue (2000).

The sinuous pockmark belt (Area 2)

Area 2 is a 3 to 4 km wide and 41 km long pockmark band, crossing the study area from the SE to the NW corner. Its southern boundary is coincident with the right bank of the Zaire canyon. Pockmarks in this area are 100 to 800 m long, with a maximum depth of over 40 m. Some pockmarks are open-ended, suggesting that they have formed from the coalescence of several smaller pockmarks. They are mainly concentrated in the central part of Area 2, along a 22 km long section. They are regularly spaced about 300 m apart, along a sinuous belt.

The high-resolution PASISAR profile (Fig. 4) crosses one of these pockmarks on the right levee of the Zaire canyon. The reflections below the pockmark appear depressed and not enhanced, in contrast to the observations made on seismic profiles in Area 1. Moreover, no inverted V-shape anomaly was detected directly beneath the depressed zone. We conclude that the down bowing of these reflections is not an artifact, but the reflectors are physically depressed and represent a chimney for ascending fluids from underlying levels to the seafloor.

At about 200 m below seafloor, the chimney branches on an ancient buried channel-levee system. Reflectors are depressed down to the palaeochannel and along the channel-levee interface. The base of the chimney is located on the left edge of the channel fill, where it seems to take root because of the lack of any deeper sound-speed anomaly. The close relationship between the pockmark and the buried palaeochannel is evident on the PASISAR profile CD, which has been performed by horizon mapping on 3D-seismic.

Mapping of the buried palaeochannel

Automatic picking of the base of the palaeochannel is difficult because of the irregular reflection patterns. To map palaeochannels, two continuous horizons with high amplitudes (Fig. 5) were combined, one within the channel fill and one within the levee system. The combination of the two horizons provides an isochronal map of the palaeochannel.

The dip map shown on Figure 6a clearly delineates the channel trend that borders the present day Zaire canyon from the SE to the NW. The sinuosity

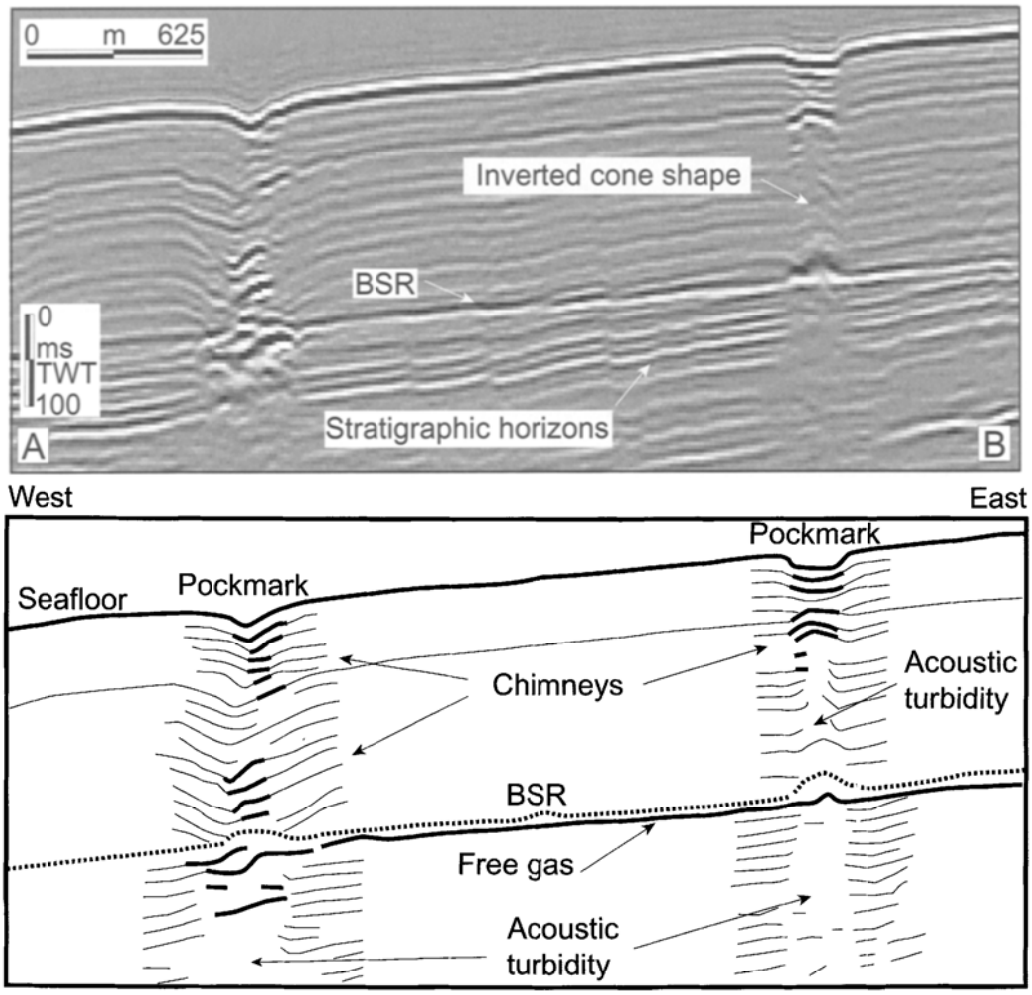

Fig. 3. Seismic profile AB in Area 1, extracted from 3D data, and interpreted line drawing. This profile crosses two pockmarks, illustrating the close relationship between seafloor features, associated chimneys and the BSR. High amplitude reflectors in chimneys are interpreted as gas-charged intervals.

of the palaeochannel is characterized by regular, smooth curves with a constant channel width of 800 m. The central axis of the palaeochannel seems to coincide with the meandering trend of pockmarks identified on the seafloor (Fig. 6b). Moreover, pockmarks within Area 2 are located above the edges of the buried channel-levee system.

Spatial characteristics of the sedimentary cover above the palaeochannel

The sedimentary cover above the palaeochannel as constrainted by using a time-to-depth empirical function by seismic-well calibration provided by Total-Fina-Elf. With this rule, the synthetic isochronal map of the palaeochannel has been converted into an isodepth map and the sediment thickness above the channel-levee system has been represented as an isopach map (Fig. 7). This map shows the general decrease of the sediment thickness, from 360 metres in the SE to 20 metres in the NW, in agreement with the sedimentation rates calculated from three cores drilled in this area during the Leg ODP 175. The sedimentation rate decreases from the eastern shallower site (site 1076) to the western deeper site (site 1075) from 15 cm/k to 10 cm/k.y (Giraudeau *et al.* 1998). This overall seaward decrease in sedimentation rate indicates the progressive disappearance of terrigenous and hemipelagic input.

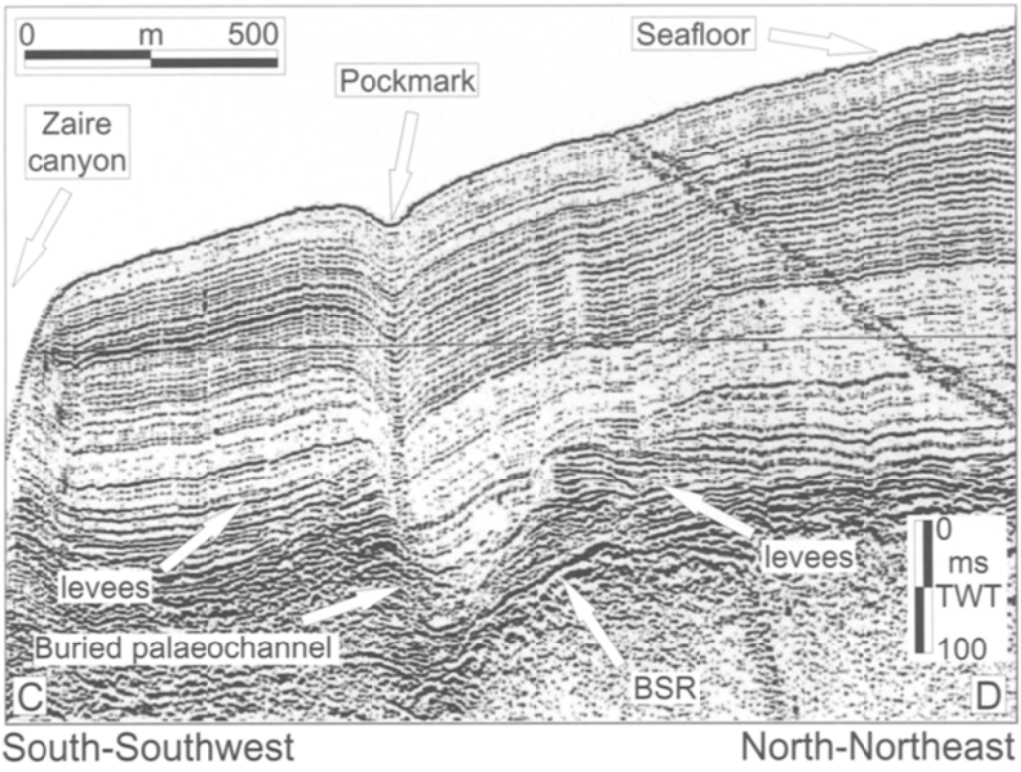

Fig. 4. PASISAR profile CD showing the close relationship between pockmarks at the seafloor in Area 2 and a buried palaeochannel. A vertically elongated zone of depressed reflectors up to 180 ms TWT below the seafloor is interpreted as a seismic chimney. No acoustic anomalies have been identified at deeper levels, suggesting that the migration of fluids started at the channel-levee interface.

Relationship between pockmarks, palaeochannel and the sedimentary cover

As previously outlined on the dip seafloor map, pockmarks are concentrated along 22 km in the central part of Area 2 (Fig. 8). Arrows indicate the real positions of pockmarks along the palaeochannel axis. The general trend of the curve presents two knick-points, which determine three individual zones highlighted by three grey backgrounds:

(1) The distal zone in the NW part of Area 2 is the zone of thinnest sediment cover. The thickness varies from 15 m to 130 m. No pockmarks have been identified on the seafloor in this zone.
(2) The central zone of Area 2 includes the majority of pockmarks. Although the thickness of overlying sediments varies from a minimum of 110 m to a maximum of 245 m, with an average of 175 m. Pockmarks only appear where the thickness of the sediment cover ranges from 130 m to 240 m.
(3) The landward zone, in the SE part of Area 2, is the zone of thickest sediments. This zone is characterized by an average thickness of the sedimentary cover ranging from 165 m to 260 m. Only four pockmarks occur in this zone, all four in places where the sediment cover is less than 240 m.

Morphological evidences for fluid seepages on seismic profiles and dip seafloor maps

Different morphological features on seismic profiles and dip seafloor maps have been observed on the three previously identified sub-zones of Area 2.

The seismic profile GH (Fig. 9) in the distal zone shows that some depressions are not located directly over the channel axis (600 m or more), but systematically located at higher bathymetric levels. This suggests that they are markers of ancient abandoned meander loops, such as in the present Zaire canyon (Babonneau *et al.* 2002). These perched meander loops show crescent-shaped depressions of about 600 m length that are progressively buried due to the

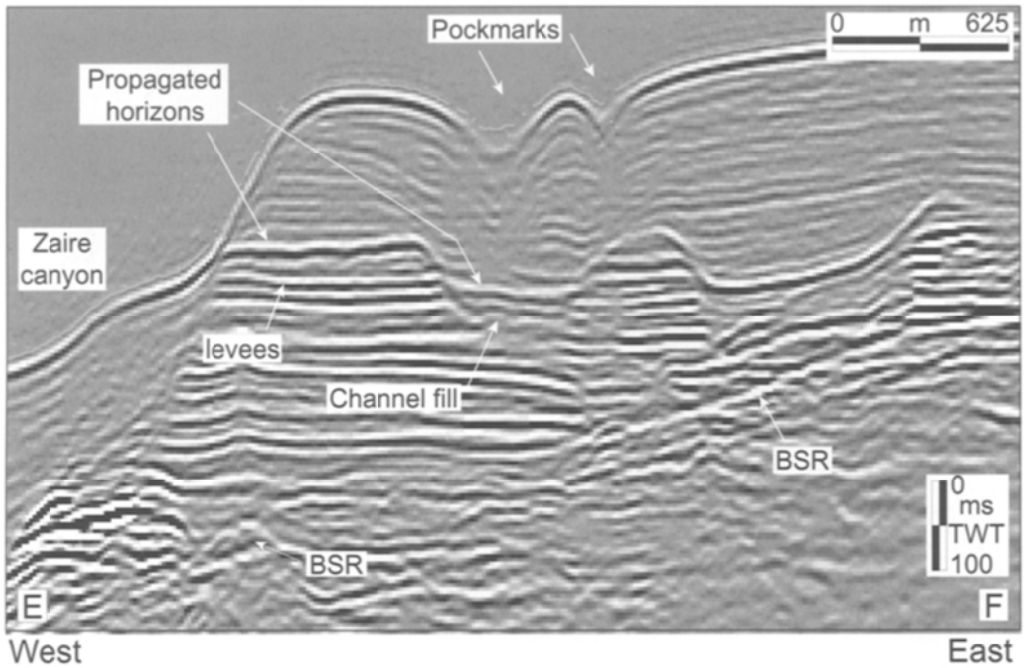

Fig. 5. Seismic profile EF in Area 2, extracted from 3D data, crossing the buried palaeochannel. This profile illustrates the difficulty to map the buried channel by automatic horizon picking. Manual picking of the base of the channel would be time-consuming. Two continuous high-amplitude horizons located near the top of the channel fill and near the top of the levees were traced to map the palaeochannel. This way, the general morphology of the palaeochannel is preserved.

upward increase of sedimentation rate. All parallel horizons above both levees of the palaeochannel are truncated near flanks of the depression and display top-lap structures, suggesting erosional or non-depositional features. Due to the presence of a constructive dome, it is suggested that both depressions are due to fluid escape, which locally prevents a normal sedimentation rate. In the central zone, the entire buried channel-levee system is pointed out by the meandering track of highly concentrated pockmarks on the seafloor (Fig. 10). It appears that their location seems to be dependent on sediment thickness above the palaeochannel. Pockmarks are mostly concentrated in the distal part of this zone, where long depressions result from the coalescence of two (or more) smaller pockmarks, suggesting a peanut-shaped geometry (i.e., composite pockmarks). In this zone, no isolated seafloor pockmarks, nor buried chimneys or fossil pockmarks have been identified on seismic sections. These morphological features indicate that fluid escape is currently active or has been recently active. In the landward zone, only four small pockmarks have been identified. However, different to the central zone, numerous buried structures such as chimneys and buried pockmarks (Long 1992) are visible on seismic sections crossing the palaeochannel (Fig. 11). They are identified on seismic profiles by depressed reflectors, horizontally sealed by slope sediments at the present day. Buried pockmarks are systematically located above channel flanks and indicate the past activity for fluid seepage above the channel-levee system. The few pockmarks visible on the modern seafloor could indicate secondary fluid migration through ancient reactivated chimneys.

Mechanical model for overpressure in a buried silty/sandy channel

The channel fill is generally characterized by a predominantly sandy/silty sediment. Stratified hemipelagic sediments cover the channel-levee system, leading to its progressive burial and compaction. Overpressure development in sedimentary basins is directly related to the types of sediment facies deposited (controlling lithology), sedimentation rate, thermal expansion of fluids, transformation of clay minerals and to hydrocarbon generation (Yu & Lerche 1996) or bacterial methanogenesis. Among these factors, sediment facies and sedimentation rates are the main factors controlling fluid pressure

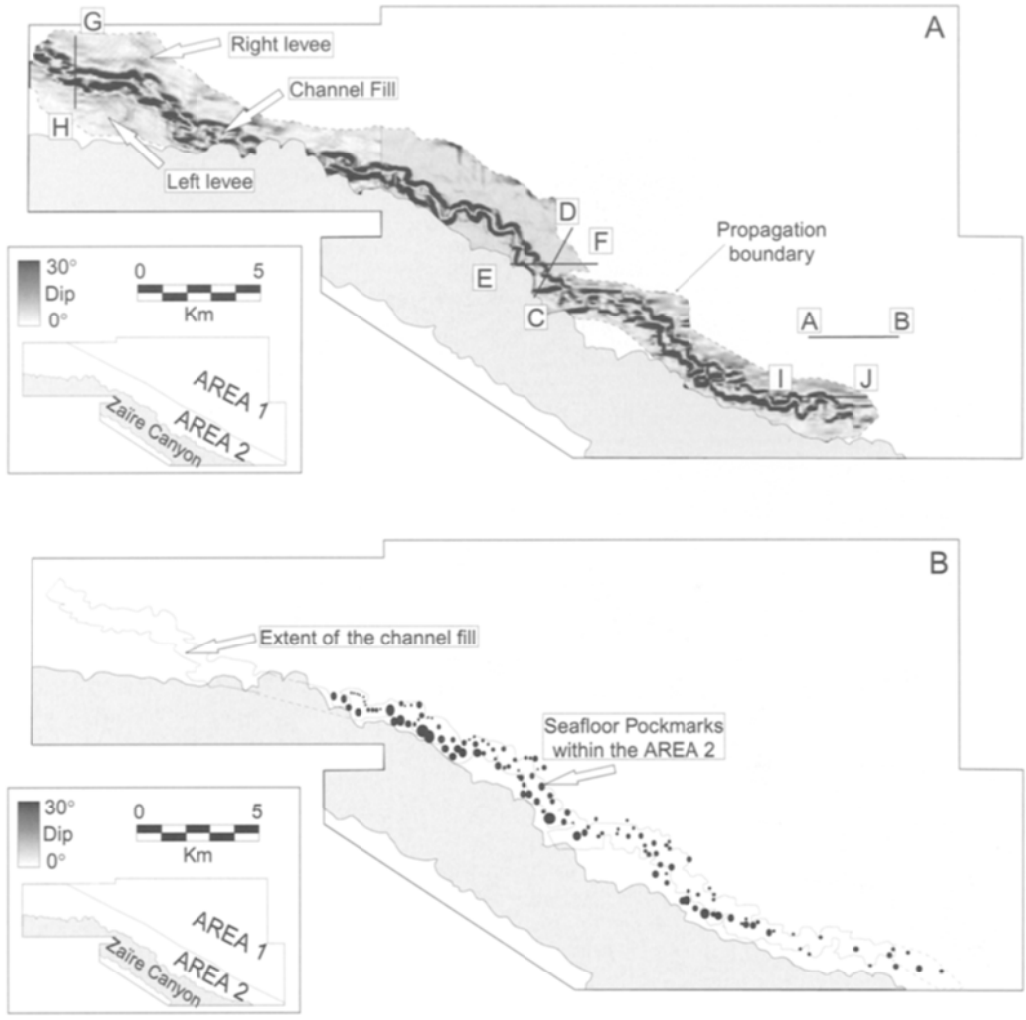

Fig. 6. A Dip map of the two mapped horizons at the level of the palaeochannel (see Fig. 5). B Spatial correlation between seafloor pockmarks and the channel extent. All pockmarks in Area 2 (black circles) occur at the channel flanks. The meandering track of pockmarks at the seafloor represents the sinuous trend of the buried palaeochannel.

development in a basin. In this case, hemipelagic mud with low permeability entraps the palaeochannel, characterized by higher permeabilities and prevents efficient dewatering of pore fluids. A rapid increase of the overburden pressure can lead to the generation of excess pore fluid pressures (Bolton & Maltman 1998), and fluids can escape from the sand/silt body through the muddy cover, creating pockmarks on seafloor (Cole *et al.* 2000). In this case, pockmarks form in fine sediments and not in sandy sediments as reported by Hovland in the North Sea (Hovland & Judd 1988).

In a sedimentary column, an elementary volume ΔV is subjected to three forces:

(1) its own weight, Fg, due to gravity:

$$Fg = \rho_{sat}.\Delta V, \quad (1)$$

where ρ_{sat} is the specific gravity (in $kN.m^{-3}$);

(2) forces of buoyancy, Fb, due to immersion in water:

$$Fb = \rho_{f}.\Delta V, \quad (2)$$

where ρ_f is the specific gravity of fluid (generally 10 $kN.m^{-3}$);

(3) seepage forces, Fs, due to fluid flow:

$$Fs = i.\ \rho_{f}.\Delta V, \quad (3)$$

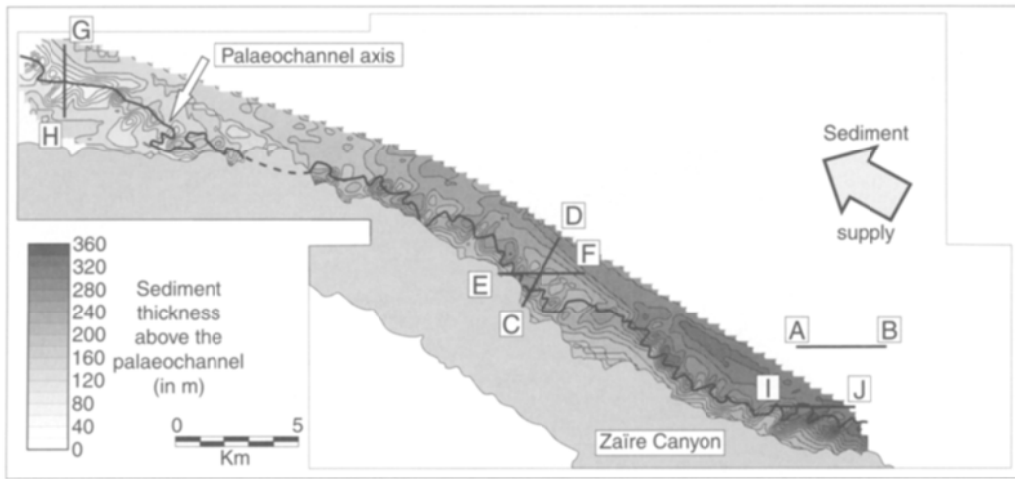

Fig. 7. Isopach map of the sediment cover of the palaeochannel. The thickness decreases from 360 m in the landward zone to 20 m in the distal zone, illustrating the progressive decrease of terrigenous sediment input.

where ρ_f is the specific gravity of fluid and i is the hydraulic gradient with $I = -\overrightarrow{Grad}\, h$, where h represents the head pressure.

Without any specific pathways where fluid may circulate and/or accumulate, pore fluids can escape up to the seafloor if sediments are fluidized: grains become suspended in fluid, which can migrate upward. Therefore, the balance between ascending forces (Fs and Fb) and descending forces (Fg) must be equal and the hydraulic gradient, i, must reach the critical gradient, i_c. For a vertical seepage, i_c is given by the following equation:

$$\rho_{sat}.dV = \rho_f.dV + i_c.\rho_f.dV$$

$$\rho' = \rho_{sat} - \rho_f \qquad (4)$$

where ρ' corresponds to the submerged gravity. The equation (1) becomes:

$$i_c = \rho' / \rho_f. \qquad (5)$$

For fluid migration up to the seafloor, a vertically critical gradient must be taken into account from the top of the palaeochannel to the seafloor:

$$i = \Delta h/L = i_c = \rho' / \rho_f \qquad (6)$$

where Δh is the variation of head pressures between the top of palaeochannel and seafloor and L represents the thickness between these two points. Einsele (1977) and Bonham (1980) showed that flow velocities during sediment compaction and the range of compaction-driven fluid flow primarily depend on thickness of the compacting sedimentary column.

During the Leg ODP175, bulk densities were measured and compiled on shipboard along each core, every 4 to 50 cm. Lithostratigraphical and magnetostratigraphical analyses conducted in the Lower Congo Basin show intercalations of hemipelagic and terrigenous deposits that can be easily correlated from site to site and sequences are regionally cross-correlated. Cores from site 1077, the nearest site from Area 2, should provide a good flashover of mechanical properties in our study area. Although sediment compressibility is reduced by several orders of magnitude with increasing effective stress during compaction (Neuzil 1980), real profiles of sediment compressibility and bulk density have not been integrated in any equation. For shallow processes of compaction, an average bulk density for the first 240 m is considered as a good approximation. With a sediment thickness less than 240 m, fluids can escape along discontinuities, such as the channel-levee interface. Above 240 m thickness, the sedimentation can seal the system, requiring an excess pore pressure for pockmark generation. Equation (4) yields an average value of 2.944 $kN.m^{-3}$ for the submerged density. Equation (6) gives a variation of head pressures, Δh, equal to 70.7 m, which is equivalent to an excess pore pressure at the top of palaeochannel of 0.707 MPa (considering g equal to 10 $m.s^{-2}$). This overpressure corresponds to the minimum excess pore pressure needed for pockmark formation with a sediment cover of 240 m.

Discussion

An excess pore pressure can be generated in a buried layer by two processes: (1) a thick deposit of fine-grained sediment with low permeabilities can create overpressure in an underlying level. In this case the sedimentation rate and associated lithologies are key

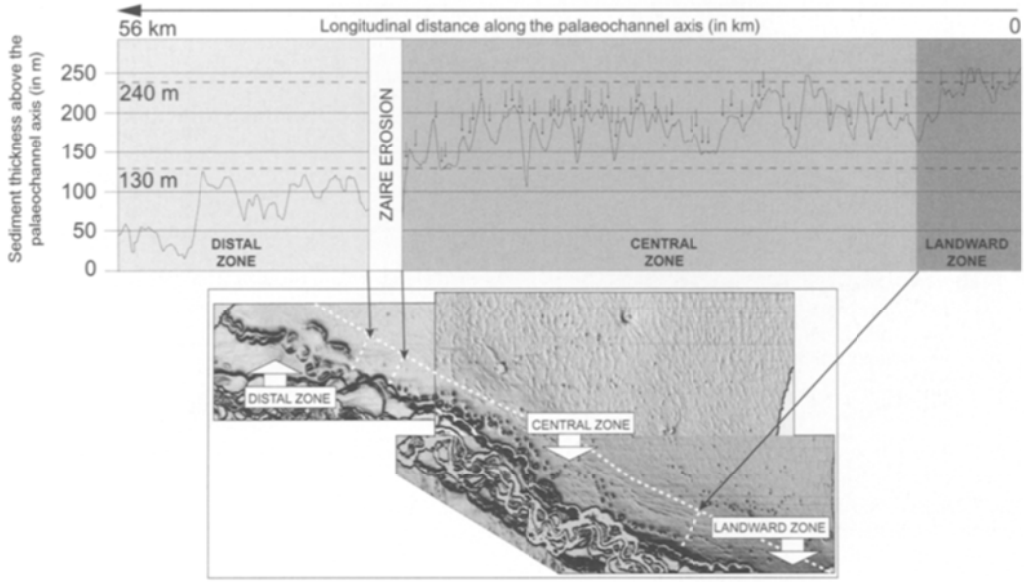

Fig. 8. Sediment thickness distribution along the palaeochannel axis. Arrows indicate the positions of pockmarks. Based on sediment thickness, three zones are identified: a distal zone (sediment cover thickness: 15–130 m), a central zone (sediment cover thickness: 130–245 m), and a landward zone (sediment cover thickness: 165–260 m). Pockmarks only occur where the thickness of the sediment cover is between 130 and 240 m.

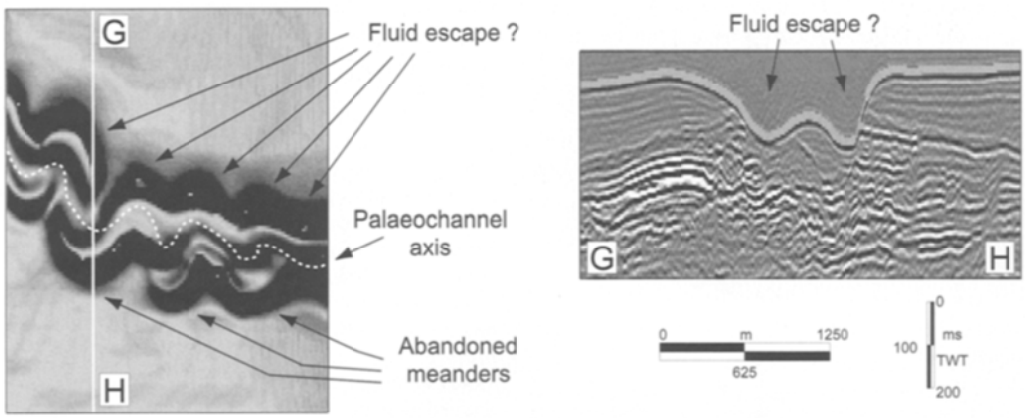

Fig. 9. Correlation between seafloor morphology and a cross-section in the distal zone of Area 2. Left: dip seafloor map. The white dashed line represents the axis of the buried palaeochannel. Right: seismic section GH across the palaeochannel (see Fig. 2 for location). Note that several curved depressions are visible on seafloor corresponding to the hemipelagic fill of abandoned meanders. They may represent areas of non-deposition due to fluid seepage.

parameters. A model described by Dugan (Dugan & Flemings 2000) predicts that significant overpressures will originate where loading is rapid. Due to the low permeabilities of the hemipelagic cover, fluids are preferentially entrapped in the sandy/silty body of the buried channel, which can lead to an excess of pore pressure and later to the up-dip migration along bedding planes, i.e. up the flanks of levees and basin fill.

Effect of the sedimentation rate for generating overpressure

The vertical stress due to an additional load is:

$$\sigma_v = \rho_{sat} d \quad (7)$$

where ρ_{sat} is the bulk density (in $kN.m^{-3}$) and d is the thickness of the new deposit (in m). The average bulk density for 240 m in the core 1077 is 12.944

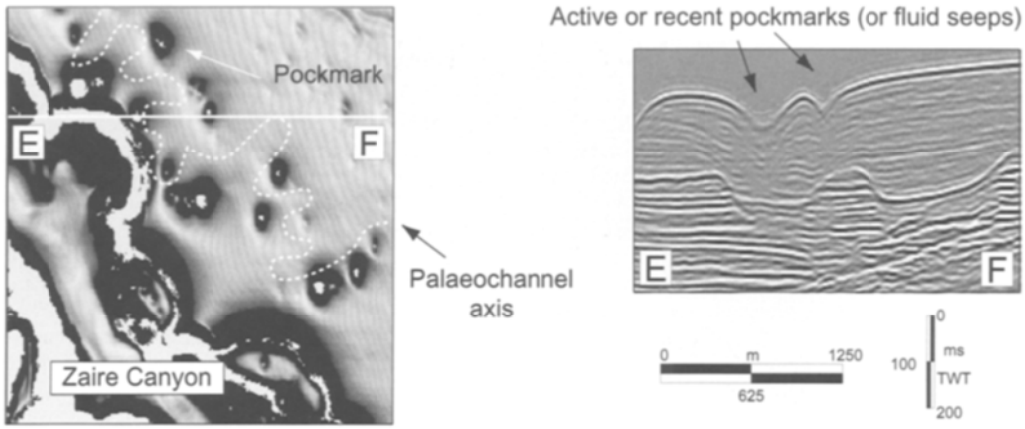

Fig. 10. Correlation between seafloor morphology and a cross-section in the central zone of Area 2. Left: seafloor dip map. The white dashed line corresponds to the palaeochannel axis. Right: seismic section EF (see Fig. 2 for location). Channel flanks are highlighted by a sinuous trend of pockmarks at the seafloor. Pockmarks and underlying chimneys seem to take root at the channel-levee interface.

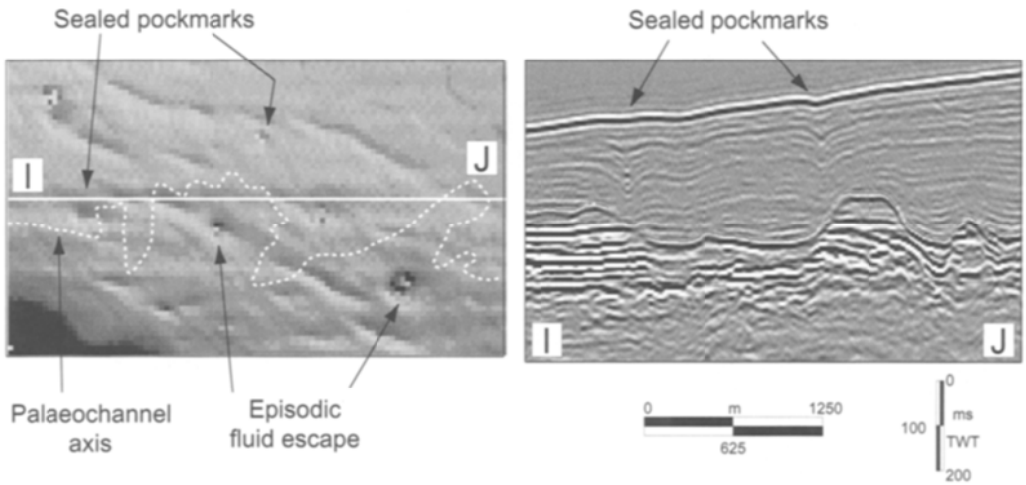

Fig. 11. Correlation between seafloor morphology and a cross-section in the landward zone of Area 2. Left: seafloor dip map. The white dashed line represent the axis of the buried palaeochannel. Right: seismic section IJ (see Fig. 2 for location). Only four pockmarks have been identified in this zone. All other pockmarks seem to be sealed. This zone may represent an area of episodic seepage due to the high sealing capacity of the hemipelagic cover.

$kN.m^{-3}$ and the vertical stress corresponding to the overpressure is 707 $kN.m^{-2}$. Equation (7) gives a value of d equal or superior to about 56 m. This thickness represents the last 56 m of the sediment cover (240 m), which has been deposited very quickly over the palaeochannel, leading to the overpressure. The dissipation time of overpressured fluids, $t_{\%}$, depends on the hydraulic diffusivity D_z (1.10^{-8} $m^2.s^{-1}$ in the study area, calculated from ODP data, ODP175 initial report, in Wefer *et al.* 1998b), on the maximum vertical distance of dissipation z (the dissipation can be performed upward or downward, so z = 240 / 2 = 120 m) and on the time factor T_v (in%):

$$t_{\%} = \frac{Tv_{\%}.(z)^2}{Dz} \qquad (8)$$

T_v is related to the consolidation rate U (in %). Values of T_v are available from pre-calibrated curves or can be expressed from a Fourier series (see Appendix for details). For a consolidation rate of 50%, $T_{v50\%} = 0.197$ and Equation (8) gives a time dissipation of 9000 years. For a consolidation rate of

99%, $T_{v99\%} = 2$, the time dissipation is 91,000 years. The average sedimentation rate at the site 1077 is about 10 cm/k.y and reaches 20 cm/k.y for the last 200000 years (Wefer *et al.* 1998*a*). Based on a maximum sedimentation rate of 20 cm/k.y, 56 m would have been deposited in 275,000 years. The overpressure would have already dissipated when the sediment thickness reached 56 m.

Thus, the sedimentation rate appears insufficient to explain an overloading effect capable of producing the excess of pressure needed to expel fluids up to the seafloor. Only repeated overflow deposits from the Zaire canyon could build up a thick sediment cover rapidly reaching 56 m. Biostratigraphical analyses of all sites in the Lower Congo Basin indicate an overall continuous hemipelagic sedimentation, characterized by the absence of (or only minor) post-depositional sediment transport. Only one thin and isolated Bouma D/E turbidite sequence has been identified (Pufahl *et al.* 1998, and site 1075 descriptions).

Fluids migration from deeper levels as a key parameter

Pockmark structures are commonly attributed to fluid venting from overpressured biogenic/thermogenic methane, oil or other pore fluids. In the slope of the Lower Congo basin, the hemipelagic sediments play the role of an impermeable seal over the turbiditic palaeochannel. If fluids migrate from underlying levels, they are preferentially entrapped in higher permeability layers, represented here by the sandy/silty linear body (Hovland & Judd 1988; Tinkle *et al.* 1988; Mann & Mackenzie 1990; Premchitt *et al.* 1992). In these conditions, the channel acts as a drainage pipe, and the supply of ascending fluid from deeper overpressured reservoir can exceed the pore pressure limit of 0.707 MPa necessary for fluidization, upward migration and pockmark formation on the seafloor. This hypothesis implies that fluids migrating up to the palaeochannel, partly originate from deep thermogenic processes (Brooks *et al.* 1999). The expected nature of fluids escaping from seafloor pockmarks should be a mixture of interstitial water, shallow biogenic gases (produced by bacterial degradation of organic matter) and thermogenic gases or oil from deep buried reservoirs. A discontinuous BSR is evident on 3D-seismic data in Area 1, directly superposed beneath deep-buried palaeochannel bodies (Figs 5 and 10). This is in contrast to Area 2, where no distinct BSR is evident beneath the shallow buried channel, indicating the lack of free gas trapped under gas hydrates or the lack of gas hydrates themselves. It is suggested that the chimneys directly expel all fluids from the channel body reservoir. Pockmark belt and associated shallow buried channel act as a by-pass zone for free gases.

Due to the sandy/silty nature of the channel fill, the overpressure is uniformly distributed along the channel body. Dugan & Flemings (2000) developed a two-dimensional model to generate overpressure, in which the geometry of the reservoir and rate of loading control lateral fluid transfer. This model predicts that significant overpressures will originate where loading is rapid. Longitudinal flow occurs in the palaeochannel because a pressure gradient exists, due to the differential loading above it. The gradient is assumed to be highly dependent on the loading geometry, the bulk compressibility and the hydraulic conductivity. The pockmark distribution on seafloor is not dependent on the location of the fluid sources under the palaeochannel, because this lateral gradient exists.

Conceptual model for fluid seepages above a shallow buried palaeochannel

Area 2 is characterized by a seaward decrease of the sedimentary cover above a shallow buried channel axis, where three sub-zones have been identified as a function of morphological features on the seafloor and on seismic sections:

(1) the distal zone displays direct fluid escape because the sedimentary cover is very thin above buried meanders;
(2) the central zone has a medium-thick cover that allows active fluid seepage creating new pockmarks or re-using ancient chimney, that can lead to vertically stacked pockmarks;
(3) the landward zone is characterized by a thick sedimentary cover; pockmarks are sealed because the rate of sedimentation exceeds the seepage forces, but fluids can periodically escape.

This pattern demonstrates that channel-related pockmarks are active over a window of sediment cover of thickness between 130 m and 240 m. This active fluid window moves basinward during time by slope progradation and pockmarks progressively mimic the palaeochannel axis (Fig. 12).

Conversely, in the landward zone, numerous fossil pockmarks and associated chimneys indicate a past activity for fluid seepage (Hovland *et al.* 1984). The thickness between the channel-levee interface and fossil pockmarks is of the same order as the present day thickness of the cover observed in the central zone of Area 2 (Fig. 10). This last observation suggests that leakage processes may stop where there is a high seal capacity of the sedimentary cover. If the mechanical model for expelling fluids

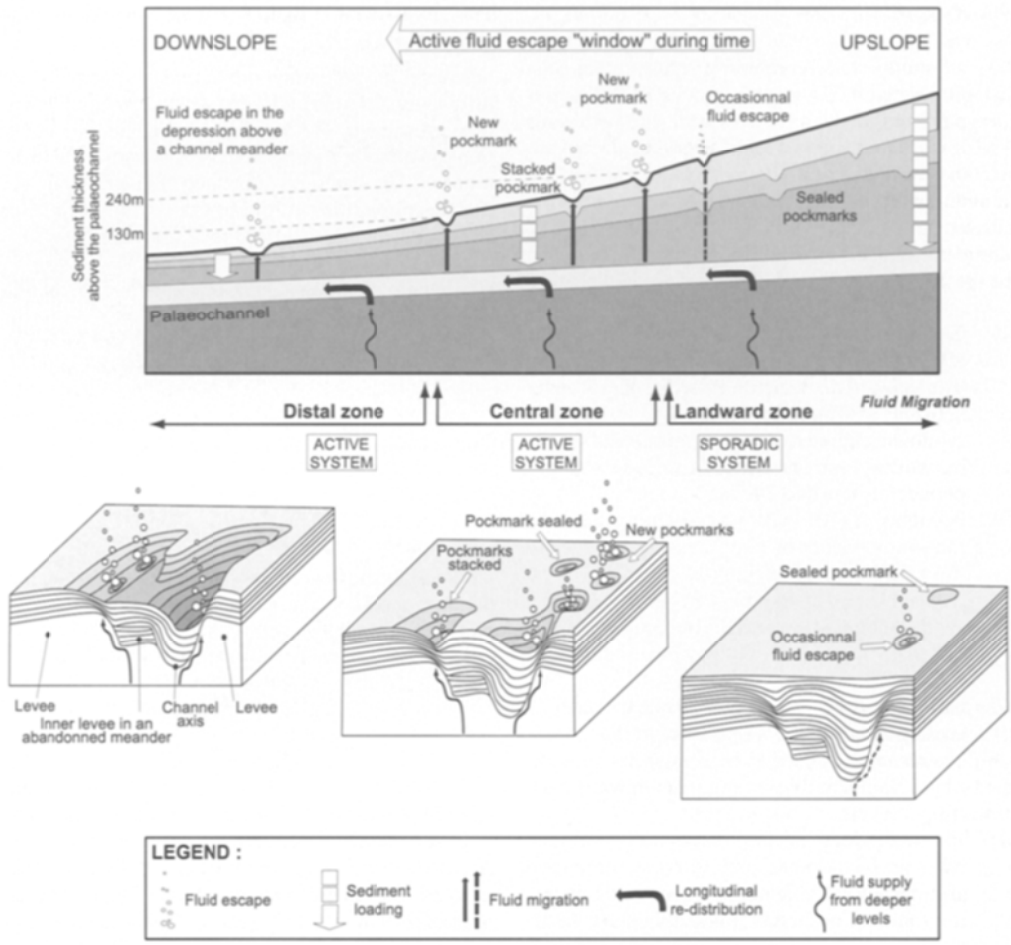

Fig. 12. Conceptual model for fluid expulsion from a sandy/silty buried channel.
Fluid escape in the landward zone is assumed to be sporadic, because of a thick sediment cover and characterized by a low pockmark density on the seafloor. Central and distal zones may be active for fluid seepage at the present day. This 'active window' moves basinward in pace with slope progradation.

from shallow buried channel is clearly evidenced by 3D seismic profiles, the spatial link with deep over pressured reservoirs remains more hypothetical. It seems that at a greater depth, a rapid porosity collapse may generate overpressure and lead to the development of tensile fractures, veins and sand injections contributing to fluid migration (Fisher *et al.* 1999). Some examples of similar features have been reported in layered strata with strong permeability contrasts from the Gulf of Mexico. In this area, the overpressured fluids from the sand layers migrate upwards in the overlying mud by fracture permeability, following the minimum principal stress (Bishop Stump & Flemings 2000; Cole *et al.* 2000). In the North Sea, buried craters have been observed at a Pliocene horizon, which may have been formed during an earlier period of sustained gas seepage.

Hydrocarbon migration pathways are largely controlled by the distribution of high permeability conduits, such as faults (Yu & Lerche 1996) and sand-rich carrier sequences and their structural dip or geometry (Burley *et al.* 2000). In particular, Cartwright (1994) and Lonergan *et al.* (1998) described thick mudstone-dominated sequences disrupted by complex arrays of small extensional faults distributed at intervals of 100–500 m. The network of faults is assumed to be produced by volumetric contraction of fine-grained sediments; it may easily drive fluids from underlying stratigraphic units up to the seafloor.

Conclusion

This integrated study combining conventional seismic profiles with 3D seismic blocks in the Lower Congo Basin showed a close relationship between a type of seafloor pockmarks and a buried palaeochannel: these pockmarks seem to take root at the channel-levee interface. They are systematically distributed on both sides of the buried channel body and mimic the meandering track of the palaeochannel on the seafloor. Six key results have been established:

(1) The buried turbiditic channel determines a horizontal drain for lateral fluid flow.
(2) The seaward decrease of the sedimentary cover activates a differential overloading responsible of down channel fluid migration and pockmarks development, when the thickness ranges between 130 m and 240 m.
(3) A value of 707 kPa was calculated as the minimum excess of pore pressure needed for fluid bursting and pockmarks formation, for a channel buried at about 240 m below seafloor.
(4) As the sedimentary wedges build up the slope, this open-window moves downward along the palaeochannel axis.
(5) Considering the sedimentation rate in the study area, the excess of pore pressure in the palaeochannel is supposed to be created by an additional fluid supply that migrates upward from deeper levels.
(6) Discontinuities in the sedimentary column, such as faults, erosional surfaces, or buried chimneys may channelize deep fluids during migration. Conversely, all sedimentary structures, such as channel bodies or sandy/silty layers, concentrate fluids before redistribution as intermediate reservoirs.

Finally, a new type of pockmark closely linked to a buried palaeochannel has been described in the Lower Congo Basin and a hydromechanical model has been proposed, which implies the mixing of shallow and deep buried reservoirs. These seismic chimneys are the spatial link between source rock, reservoir trap and shallow-gas anomalies; their detection may be indicative of both potential zones of geohazards and deeper prospective reservoirs (Heggland 1998; Aminzadeh *et al.* 2001; Tingdahl *et al.* 2001).

Appendix

The process of consolidation is directly linked to the rate of excess pore pressure dissipation. The one-dimensional consolidation theory is governed by the following differential equation (Terzaghi 1943):

$$D_z \frac{\partial^2 u}{\partial z^2} = \frac{\partial u}{\partial t} \tag{9}$$

where u is the pore water pressure, D_z is the hydraulic diffusivity, t is time and z denotes the position where u is determined. The Terzaghi's consolidation equation can be solved using analytical or numerical techniques. The solution obtained depends on the boundary conditions. For our case, with a soil layer of height, 2H, the boundary conditions are:

(a) complete drainage at top and bottom of the layer; $u = 0$ at $z = 0$ and $z = 2H$;
(b) the initial excess pore water pressure $\Delta u = u_I$ is equal to the applied stress increment $\Delta\sigma$.

The solution is obtained as a Fourier series, which can be expressed in the following form:

$$U_z = 1 - \sum_{n=0}^{\infty} f_1\left(\frac{z}{H}\right) f_2(T_V) \tag{10}$$

where U_z is the degree of consolidation at time, t, at depth z, and T_V is a non-dimensional time factor. U_z and T are given by:

$$T_v = D_z \frac{t}{H_{dr}^2} \tag{11}$$

$$U_z = -\frac{u}{u_i} \tag{12}$$

where H_{dr} is the length of the longest drainage path.

Based on the numerical solution of equation (10), and in order to define the time factor Tv as a function of the degree of consolidation U_z, Casagrande (1936) and Taylor (1948) determine a 'pre-calibrated' curve concerning the Time factor, T_v, which is given by the following equations:

$$U_z > 60\%$$
$$Tv = 1.78 - 0.933\log(100 - U_z(\%)) \tag{13}$$

$$U_z > 60\% \quad T_v = \frac{\pi}{4}\left(\frac{U_z(\%)}{100}\right)^2. \tag{14}$$

From equations (11), (13) and (14) and for a given hydraulic diffusivity D_z and for a given drainage path H_{dr}, it is possible to evaluate the time t needed to obtain a specified degree of consolidation U_z.

This work was largely improved by the data of the ZAIANGO project, co-sponsored by IFREMER and TotalFina-Elf. Authors are very grateful to A. Morash head of the Deep Offshore Project at TFE; and Bruno Savoye head of the ZAIANGO project at IFREMER, for their financial support and data supplies. M. Hovland, P. Vogt and an anonymous reviewer are gratefully acknowledged for their critical reviews and their suggestions. We warmly thank P. Van Rensbergen for his careful English edit and N. Babonneau for useful comments concerning the Zaire canyon.

References

ABRAMS, M.A. 1992. Geophysical and geochemical evidence for subsurface hydrocarbon leakage in the Bering Sea, Alaska. *Marine and Petroleum Geology*, **9**, 208–221.

ABRAMS, M.A. 1996. Distribution of subsurface hydrocarbon seepage in near-surface marine sediments. *In:* SCHUMACHER, D. & ABRAMS, M.A. (eds) *Hydrocarbon Migration and its near-surface expression. American Association of Petroleum Geologists Memoir*, **66**, 1–14.

AMINZADEH, F., DE GROOT, P.F., BERGE, T. & VALENTI, G. 2001. Using gas chimneys as an exploration tool. *World Oil*, May 2001, 50–56.

BABONNEAU, N., SAVOYE, B., CREMER, B. & KLEIN, B. 2002. Morphology and architecture of the present canyon and channel system of the Zaire deep-sea fan. *Marine and Petroleum Geology*, **19**, 445–467.

BARAZA, J., ERCILLA, G. & NELSON, C.H. 1999. Potential geologic hazards on the eastern Gulf of Cadiz slope (SW Spain). *Marine Geology*, **155**, 191–215.

BARTEK, L.R., VAIL, P.R., ANDERSON, J.B., EMMET, P.A. & WU, S. 1991. Effect of Cenozoic ice sheet fluctuations in Antartica on the stratigraphic signature of the Neogene. *Journal of Geophysical Research*, **96**, 6753–6778.

BISHOP STUMP, B. & FLEMINGS, P.B. 2000. Overpressure and fluid flow in dipping structures of the offshore Gulf of Mexico (E.I. 330 field). *Journal of Geochemical Exploration*, **69–70**, 23–28.

BOE, R., RISE, L. & OTTESEN, D. 1998. Elongate depressions on the southern slope of the Norwegian trench (Skagerrak): morphology and evolution. *Marine Geology*, **146**, 191–203.

BOLTON, A. & MALTMAN, A. 1998. Fluid-flow pathways in actively deforming sediments: the role of pore fluid pressures and volume change. *Marine and Petroleum Geology*, **15**, (4), 281–297.

BONHAM, L.C. 1980. Migration of hydrocarbons in compacting basins. *American Association of Petroleum Geologists Bulletin*, **64**, 549–567.

BRICE, S.E., COCHRAN, M.D., PARDO, G. & EDWARDS, A.D. 1982. Tectonics and Sedimentation of the South Atlantic Rift Sequence: Cabinda, Angola. *Studies. In:* DRAKE, W.A. (ed.) *Continental Margin Geology. American Association of Petroleum Geologists Memoir*, **34**, 5–18.

BROOKS, J.M., BRYANT, W.R., BERNARD, B.B. & CAMERON, N.R. 1999. *The nature of gas hydrates on the Nigerian Continental Slope. Abstract book of the Third international conference of gas hydrates (18–22 july)*, Park City, Utah.

BROWN, A. 2000. Evaluation of possible gas microseepage mechanisms. *American Association of Petroleum Geologists Bulletin*, **84** (11), 1775–1789.

BURLEY, S.D., CLARKE, S., DODDS, A., FRIELINGSDORF, J., HUGGINS, P., RICHARDS, A., WARBURTON, I.C. & WILLIAMS, G. 2000. New insights on petroleum migration from the application of 4D basin modelling in oil and gas exploration. *Journal of Geochemical Exploration*, **69–70**, 465–470.

CARTWRIGHT, J.A. 1994. Episodic basin-wide hydrofracturing of overpressured Early Cenozoic mudrock sequences in the North Sea Basin. *Marine and Petroleum Geology*, **11** (5), 587–607.

CASAGRANDE, A. 1936. Characteristics of cohesionless soils affecting the stability of slopes and earth fills. *Journal of Boston Society of Civil Engineers*, **23**, 13–32.

COLE, D., STEWART, S.A. & CARTWRIGHT, J.A. 2000. Giant irregular pockmark craters in the Palaeogene of the Outer Moray Firth Basin, UK North Sea. *Marine and Petroleum Geology*, **17**, 563–577.

COOPER, C.K. 1999. Ocean currents offshore Northern Angola. *Proceedings Offshore Technology Conference* Paper 10749, Houston, Texas, May 3–6.

DROZ, L., RIGAUT, F., COCHONAT, P. & TOFANI, R. 1996. Morphology and recent evolution of the Zaire turbidite system (Gulf of Guinea). *Geological Society of America Bulletin*, **108** (3), 253–269.

DUGAN, B. & FLEMINGS, P.B. 2000. The New Jersey margin: compaction and fluid flow. *Journal of Geochemical Exploration*, **69–70**, 477–481.

EICHUBL, P., GREENE, H.G., NAEHR, T. & MAHER, N. 2000. Structural control of fluid flow: offshore fluid seepage in the Santa Barbara Basin, California. *Journal of Geochemical Exploration*, **69–70**, 545–549.

EINSELE, G. 1977. Range, velocity and material flux of compaction flow in growing sedimentary sequences. *Sedimentology*, **24**, 639–655.

FISHER, Q.J., CASEY, M., BEN CLENNELL, M. & KNIPE, R.J. 1999. Mechanical compaction of deeply buried sandstones of the North Sea. *Marine and Petroleum Geology*, **16**, 605–618.

GIRAUDEAU, J., CHRISTENSEN, B.A., HERMELIN, O., LANGE, C.B., MOTOYAMA, I. & Shipboard Scientific Party. 1998. Biostratigraphic age models and sedimentation rates along the southwest African Margin. *In:* WEFER, G., BERGER, W.H., RICHTER, C. *et al.* (eds) *Proceedings of the Ocean Drilling Program.* Initial Reports, **175**, 543–546.

GRAUE, K. 2000. Mud volcanoes in deepwater Nigeria. *Marine and Petroleum Geology*, **17**, No. 8, 959–974.

HEGGLAND, R. 1997. Detection of gas migration from a deep source by the use of exploration 3D seismic data. *Marine Geology*, **13**, 41–47.

HEGGLAND, R. 1998. Gas seepage as an indicator of deeper prospective reservoirs. A study based on exploration 3D seismic data. *Marine and Petroleum Geology*, **15**, 1–9.

HEMPEL, P., SPIESS, V. & SCHREIBER, R. 1994. Expulsion of shallow gas in the Skagerrak- Evidence from subbottom profiling, seismic, hydroacoustical and geochemical data. *Estuarine, Coastal and Shelf Science*, **38**, 583–601.

HOVLAND, M. 1981. Characteristics of pockmarks in the Norwegian trench. *Marine Geology*, **39**, 103–117.

HOVLAND, M., JUDD, A.G. & KING, L.H. 1984. Characteristic features of pockmarks on the north sea floor and scotian shelf. *Sedimentology*, **31**, 471–480.

HOVLAND, M. & JUDD, A. 1988. *Seabed pockmarks and seepages*. Graham and Trotman, London.

HOVLAND, M., GALLAGHER, J.W., CLENNELL, M.D. & LEKVAM, K. 1997. Gas hydrate and free gas volumes in marine sediments: Example from the Niger Delta front. *Marine and Petroleum Geology*, **14** (3) 245–255.

JANSEN, J.H., VAN WEERING, T.C.E., GIELES, R. & VAN IPRESEN, J. 1984. Middle and Late Quaternary oceanography and climatology of the Zaire-Congo fan and the adjacent eastern Angola Basin. *Netherlands Journal of Sea Research*, **17**, 201–249.

JOSENHANS, H.W., KING, L.H. & FADER, G.B. 1978. A side-scan sonar mosaic of pockmarks on the Scotian shelf. *Canadian Journal Earth Science*, **15**, 831–840.

KELLEY, J.T., DICKSON, S.M., BELKNAP, D.F., BARNHARDT, W.A. & HENDERSON, M. 1994. Giant sea-bed pockmarks: Evidence for gas escape from Belfast Bay, Maine. *Geology*, **22**, 59–62.

KIDD, G.D. 1999. Fundamentals of 3D seismic volume visualization. *Proceedings Offshore Technology Conference* Paper 11054, Houston, Texas, May 3–6, 823–836.

KING, L.H. & MACLEAN, B. 1970. Pockmarks on the Scotian shelf. *Geological Society of America Bulletin*, **81**, 3141–3148.

LONERGAN, L., CARTWRIGHT, J. & JOLLY, R. 1998. The geometry of polygonal fault systems in Tertiary mudrocks of the North Sea. *Journal of Structural Geology*, **20**, (5), 529–548.

LONG, D. 1992. Devensian Late-glacial gas escape in the central North sea. *Continental Shelf Research*, **12** (10), 1097–1110.

MANN, D.M. & MACKENZIE, A.S. 1990. Prediction of pore fluid pressures in sedimentary basins. *Marine and Petroleum Geology*, **7**, 55–65.

MARTON, L.G., TARI, G.C. & LEHMANN, C.T. 2000. Evolution of the Angola passive Margin, West Africa, with Emphasis on Post-Salt Structural Styles. *In:* MORIAK, W. & TALWANI, M. (eds) *Atlantic Rifts and Continental Margins*. Washington, DC, American Geophysical Union, 129–149.

Neuzil, C.E. 1980. Groundwater flow in low permeability environments. *Water Resources Research*, **22**, 1163–1195.

ORANGE, D.L., GREENE, H.G., REED, D., MARTIN, J.B., MCHUGH, C.M., RYAN, W.B.F., MAHER, N., STAKES, D. & BARRY, J. 1999. Widespread fluid expulsion on a translational continental margin: Mud volcanoes, fault zones, headless canyons, and organic-rich substrate in Monterey Bay, California. *Geological Society of America Bulletin*, **111**, 992–1009.

PREMCHITT, J., VON RAD, N.S., TO, P., SHAW, R. & JAMES, J.W.C. 1992. A study of gas in marine sediments in Hong Kong. *Continental Shelf Research*, **12**, 1251–1264.

PUFAHL, P. K., MASLIN, M.A., ANDERSON, L., BRÜCHERT, V., JANSEN, F., LIN, H., PEREZ, M., VIDAL, L. & Shipboard Scientific Party. 1998. Lithostratigraphic summary for LEG 175: Angola-Benguela upwelling system. *In:* WEFER, G., BERGER, W.H., RICHTER, C. *et al.* (eds). *Proceedings of the Ocean Drilling Program*. Initial reports, **175**, 533–542.

REYRE, D. 1984. Petroleum Characteristics and geological evolution of a passive margin. Example of the Lower Congo-Gabon Basin. *Bulletin du Centre de Recherche Exploration Production Elf Aquitaine*, **8** (2), 303–332.

SAVOYE, B., LEON, P., DE ROECK, Y.H., MARSSET, B., LOPES, L. & HERVEOU, J. 1995. PASISAR: a new tool for near-bottom very-high resolution profiling in deep water. *First Break*, **13** (6), 253–258.

SAVOYE, B., COCHONAT, P., *et al.* 2000. Structure et évolution récente de l'éventail turbiditique du Zaire: premier résultats scientifiques des missions d'exploration ZAIANGO 1 et 2 (Marge Congo-Angola). *Comptes-Rendus de l'Académie des Sciences de la Terre et des Planètes*, **331**, 211–220.

SERANNE, M., SEGURET, M. & FAUCHIER, M. 1992. Seismic super-units and post-rift evolution of the continental passive margin of southern Gabon. *Bulletin de la Société Géologique de France*, **163**, 135–146.

SERANNE, M. 1999. Early Oligocene stratigraphic turnover on the west Africa continental margin: a signature of the Tertiary greenhouse-to-icehouse transition ?, *Terra Nova*, **11** (4), 135–140.

SHAW, J., COURTNEY, R.C. & CURRIE, J.R. 1997. Marine geology of St. George's Bay, Newfoundland, as interpreted from multibeam bathymetry and back-scatter data. *Geo-Marine Letters*, **17**, 188–194.

SHIPLEY, T.H., HOUSTON, M., BUFFLER, H.R.T., SHAUB, F.J., MCMILLEN, K.J., LADD, J.W., WORZEL, J.L. 1979. Seismic evidence for widespread possible occurrence of gas-hydrate horizons or continental slopes and rises. *American Association of Petroleum Geologists Bulletin*, **63**, 2204–2213.

SOLHEIM, A. & ELVERHOI, A. 1993. Gas-related sea floor craters in the Barents Sea. *Geo-Marine Letters*, **13**, 235–243.

SOTER, S. 1999. Macroscopic seismic anomalies and submarine pockmarks in the Corinth-Patras rift, Greece. *Tectonophysics*, **308**, 275–290.

STEWART, S.A. 1999. Seismic interpretation of circular geological structures. *Petroleum Geoscience*, **5**, 273–285.

TAYLOR, D.W. 1948. Fundamentals of soil mechanics. John Wiley, New York.

TAYLOR, M.H., DILLON, W.P. & PECHER, I.A. 2000. Trapping and migration of methane associated with the gas hydrate stability zone at the Blake Ridge Diapir: new insights from seismic data. *Marine Geology*, **164**, 79–89.

TERZAGHI, K. 1943. Theoretical soil mechanics, John Wiley, New York.

TINGDAHL, K.M., BRIL, A.H. & DE GROOT, P.F. 2001. Improving seismic chimney detection using directional attributes. *Journal of Petroleum Science and Engineering*, **29**, 205–211.

TINKLE, A.R., WENER, K.R., MEEDER, C.A., HUFF, J.F., JOHNS, D.M. & MAY, J.A. 1988. Seismic no-data zone, offshore Mississippi delta: Part I – acoustic characterization. *Proceedings Offshore Technology Conference*, Houston, Texas, May 2–5, **5753**, 65–74.

UCHUPI, E. 1992. Angola Basin: Geohistory and Construction of the Continental Rise. *In:* DE GRACIANSKY, P.A. *Geologic Evolution of Atlantic Continental Rifts*. Nostrand Reinhold, New York, 77–99.

UENZELMANN-NEBEN, G. 1998. Neogene sedimentation history of the Congo Fan. *Marine and Petroleum Geology*, **15**, 635–650.

VOGT, P.R., GERDNER, J., CRANE, K., SUNDVOR, E., BOWLES, F. & CHERKASHEV, G. 1999. Ground-Truthing 11- to 12-kHz side-scan sonar imagery in the Norwegian + Greenland Sea: Part II: Probable diapirs on the Bear Island fan slide valley margins and the Vöring Plateau. *Geo-Marine Letters*, **19** (1–2), 111–130.

WEFER, G., BERGER, W.H., RICHTER, C. & Shipboard Scientific Party 1998*a*. Facies patterns and authigenic minerals of upwelling deposits off southwest Africa. *In:* WEFER, G., BERGER, W. H., RICHTER, C. *et al. Proceedings of the Ocean Drilling Program*. Initial Reports, **175**, 487–504.

WEFER, G., BERGER, W.H., RICHTER, C. *et al.* 1998*b*. Leg ODP 175, Initial Reports.

WERNER, F. 1978. Depressions in mud sediments (Eckernfoerde Bay, Baltic Sea) related to sub-bottom and currents. *Meyniana*, **30**, 99–104.

WHITICAR, M.J. & WERNER, F. 1981. Pockmarks: Submarine vents of natural gas or freshwater seeps? *Geo-Marine Letters*, **1**, 193–199.

YU, Z. & LERCHE, I. 1996. Modelling abnormal pressure development in sandstone/shale basins. *Marine and Petroleum Geology*, **13** (2), 179–193.

YUN, J.W., ORANGE, D.L. & FIELD, M.E. 1999. Subsurface gas offshore of northern California and its link to submarine geomorphology. *Marine Geology*, **154**, 357–368.